RSC Advances

RSC Publishing

PAPER

View Article Online
View Journal

Amine intercalated clay surfaces for microbial cell immobilization and biosensing applications†

Cite this: DOI: 10.1039/c3ra40335a

Bilal Demir,[a] Muharrem Seleci,[a] Didem Ag,[a] Serdar Cevik,[b] Esra Evrim Yalcinkaya,*[c] Dilek O. Demirkol,[a] Ulku Anik[b] and Suna Timur*[a]

Received 22nd January 2013,
Accepted 1st March 2013

DOI: 10.1039/c3ra40335a

www.rsc.org/advances

Trimethylamine (TM) intercalated montmorillonite (Mont) clay was prepared and characterized using X-ray diffraction, Fourier transform infrared spectroscopy, zeta potential and thermal gravimetric measurements. *Gluconobacter oxydans* cells were immobilized on the micro-structured matrix and used in microbial sensor applications. Sensor responses were based on the respiratory activity of the cells and the consumption of oxygen was monitored at −0.7 V (*vs.* Ag/AgCl and platinum electrodes) by using glucose as a substrate. Stabilization of the bacteria was performed on the Mont using glutaraldehyde. Optimization of the TM-Mont/*G. oxydans* sensor and examination of the electrochemical mechanism were carried out in a batch system. Measurements concerning analytical characteristics, operational stability, repeatability and substrate specificity depending on the carbon source in the culture were investigated in a flow injection analysis (FIA) system. Linear ranges were found between 0.15 and 5.0 mM for the batch mode and 0.1 and 5.0 mM for the FIA system, respectively. Finally, real samples were analyzed and were compared with the results of a spectrophotometric method as reference.

Published on 07 March 2013 on http://pubs.rsc.org | doi:10.1039/C3RA40335A
Downloaded by Ege Universitesi on 03/04/2013 14:13:59.

Introduction

Clays have been widely exploited for biosensor design[1] and enzyme immobilization. Due to their mechanical and thermal stabilities, chemical inertness, well-defined layered structures, and ion-exchange properties, these materials have become versatile and inexpensive matrices for modifying sensor surfaces.[2] Typically clay minerals are layered silicates belonging to the same general family of 2 : 1 layered or phyllosilicates that include vermiculites and smectites such as montmorillonite (Mont), hectorite, saponite, beidellite, stevensite and nontronite. Mont has a central octahedral sheet of alumina fused between two external silica tetrahedral sheets and oxygen which is from the octahedral sheet and is also a tetrahedral silica. Isomorphic substitution within the layers (for instance, Al^{3+} replaced by Mg^{2+} or Fe^{2+}) generates negative charges defined through the charge exchange capacity. For Mont, this value is between 0.9–1.2 meq/g which could be varied depending on the mineral origin. In its pristine form, the excess negative charge is balanced by hydrated cations (Na^{+}, Li^{+}, Ca^{2+}) which exist in the interlayer.[3] However, pristine clay minerals can suffer from poor selectivity and restricted adsorption capacity. These limitations can be overcome by functionalization of these materials with specific organic groups like amines. As a result, organic–inorganic hybrid materials with new patterns of reactivity, selectivity or sensitivity have been formed where they can also be used to form thin films onto an electrode surface.[4]

The usage of microbial cells provides several advantages. Enzymes inside these cells don't need to be purified and can be regenerated in natural conditions since cofactors and coenzymes are already in the cell.[5] Microbial biosensors are especially attractive for the analyses of biological oxygen demand, toxic agents and assimilable sugars.[6] *Gluconobacter oxydans* (*G. oxydans*) is an obligate aerobe, which has a respiratory type of metabolism that uses oxygen as the terminal electron acceptor. It is a gram negative bacterium belonging to the family *Acetobacteraceae*. *G. oxydans* is industrially important and has the capacity to produce L-sorbose from D-sorbitol; D-gluconic acid from D-glucose; and dihydroxyacetone from glycerol by using pyrrolo quinoline quninone-dependent membrane dehydrogenases.[7] In addition, localization of the key metabolic enzymes facilitates the access of substrates to catalytic centers of enzymes.[8] Besides this, it has a fast and high oxidation efficiency.[9] Hence, the *G. oxydans* genus is regarded as an ideal component for the fabrication of whole cell biosensing systems.[9] Many *G. oxydans* based microbial sensors using various immobilization materials like conducting polymers,[10] chitosan and nanocomposites as carbon nanotubes[11,12] have been reported, previously. Some

[a]*Ege University Faculty of Science Biochemistry Department, 35100 Bornova-Izmir, Turkey. E-mail: suna.timur@ege.edu.tr; Fax: +902323115485; Tel: +902323112455*
[b]*Mugla Sitki Kocman University Faculty of Science, Chemistry Departmen, Kotekli-Mugla, Turkey*
[c]*Ege University Faculty of Science Chemistry Department, 35100 Bornova-Izmir, Turkey*

† Electronic supplementary information (ESI) available. See DOI: 10.1039/c3ra40335a

Table 1 Some features of *Gluconobacter oxydans* biosensors in the literature

Elc.	Sub.	Imm. Method.	Lin. R.	Sens.	Op. Stab.	Ref.
GE	Glc	Adsorption on CP	0.5–2.0 mM	8.850 μA mM^{-1} cm^{-2}	16.7% decrease after 4 h	13
GCE	Glc	CHIT-Fc hybrid	2.5–25 mM	0.778 μA mM^{-1} cm^{-2}	15% decrease after 3 h	14
GCE	EtOH	Depositing with CNT	10 μM–1.0 mM	74 μA mM^{-1} cm^{-2}	1.7% decrease after 43 h	12
GE	Glc	Sol–Gel/CHIT/GNPs	0.5–2.0 mM	1.598 μA mM^{-1} cm^{-2}	21% decrease after 5 h	15
GCE	EtOH	DM with a silicone rubber O-ring	10 μM–1.5 mM	5.290 μA mM^{-1} cm^{-2}	Slow decrease after 72 h	16 *FIA*
GE	Glc	CNT-modified CHIT	0.05–1.0 mM	16.42 μA mM^{-1} cm^{-2}	15% decrease after 5 h	11
GDE	Glc	ORP with a silicone rubber O-ring	0.25–2.0 mM	—	50% decrease after 3 h	17
CE	Xyl	Adsorption on ChrP	0.5–20 mM	—	—	18
GCE	EtOH	CAM	2.0–270 μM	12.38 μA mM^{-1} cm^{-2}	75% after 4.5 h	19
GCE[a]	1,3-PD	ORP with a silicon rubber O-ring	0.8 mg L^{-1}–1.5 g L^{-1}	28.2 μA mol^{-1}	70% decrease after 10 h	20
GCE	Glc	Adsorption on TM-Mont	0.15–5.0 mM	0.283 μA mM^{-1} cm^{-2}	27.1% decrease after 3 h	This work *FIA*
GCE	Glc	Adsorption on TM-Mont	0.1–5.0 mM	1.850 μA mM^{-1} cm^{-2}	—	This work *batch*
GCE	Gly	Adsorption on TM-Mont	0.5–10 mM	0.113 μA mM^{-1} cm^{-2}	—	This work *FIA*

[a] Elc: Electrode, Sub: Substrate, Imm. Met.: Immobilization method, Lin. R.: Linear Range, Sens: Sensitivity, Op. Stab.: Operational Stability, CE: Clark-type Electrode, GE: Graphite Electrode, GDE: Gold Disk electrode, GCE: Glassy Carbon electrode, CP: Conducting Polymer, CNT: Carbon nanotube, CHIT: Chitosan, Fc: Ferrocen, ORP: Osmium Redox Polymer, FIA: Flow Injection Analysis, ChrP: Chromatographic Paper, CAM: Cellulose Acetate Membrane, 1,3-PD: 1,3-Propanediol, DM: Dialysis membrane, [a]: Diameter of GCE is reported as 3.0 mm.

Published on 07 March 2013 on http://pubs.rsc.org | doi:10.1039/C3RA40335A
Downloaded by Ege Universitesi on 03/04/2013 14:13:59.

analytical features of *G. oxydans* biosensors are summarized in Table 1.

Till now, clays have been used together with various bacteria for different operations such as bioremediation and bioreactor processes.[21–24] Clay minerals build up a reservoir of K^+, Na^+, Ca^{2+}, Mg^{2+}, Al^{3+} and NH_4^+ for cell adhesions.[25] Moreover, the usage of clay structures in biomolecule immobilization on the sensor surfaces is cheap, fast and easy.[26] Mont and laponite are widely used for the fabrication of electrochemical enzymatic biosensors.[27,28] However little have known about microbial clay biosensor except in a study in which palygorskite and acclimated mixed bacteria was used for the lactate analysis.[29]

We describe here the usage of trimethylamine (TM) intercalated Mont as the immobilization matrix for microbial biosensor fabrication. As far as we know, this work is the first work that includes a combination of a bacteria and clay matrix as a model for a clay based electrochemical biosensor. Glutaraldehyde (GA) and bovine serum albumin (BSA) were also added to the medium to stabilize the biofilm layer as already used in previous reports on the investigation of enzyme based biosensors.[30,31] The TM-Mont/*G. oxydans* biosensor was optimized and characterized. The optimized system was also successfully applied in a flow injection analysis (FIA) system.

Experimental

Biological Material

The strain of *G. oxydans* DSMZ 2343 was obtained from the German Collection of Microorganisms and Cell Cultures (Braunschweig, Germany; www.dsmz.de) and was sub-cultured in media containing (in g L^{-1}): D-(+)-glucose, 100; yeast extract, 10; calcium carbonate, 20; agar, 20. Then, cells were cultivated aerobically in shake flasks on a rotary shaker (175 rpm) at 28 °C, in media containing (in g L^{-1}): yeast extract, 5.0; carbon source: glucose, 5.0.[19] Cells at late exponential phase were harvested by centrifugation at 4000 rpm for 5 min. Then, washed with 0.9% NaCl and re-centrifuged. The obtained cellular paste was used for biosensor construction. Cell growth was followed spectrophotometrically by monitoring the optical density at 600 nm.[32]

Reagents

D-(+)-glucose, BSA, glycerol, glutaraldehyde solution (25%, v/v) were purchased from Sigma Chem. Co. (St. Louis, MO, USA; www.sigmaaldrich.com). Yeast extract was purchased from Oxoid (Hampshire, England; www.oxoid.com). The Mont was obtained from West Anatolia. It was purified from bentonite before use. Particles <1.5 mm in diameter were obtained by sedimentation (ion-exchange capacity; 92 meq 100 g^{-1}). TM, dimethylamine (DM) and methylamine (M) were purchased from Fluka.

Apparatus

PalmSens Potentiostat (Palm Instruments, Houten, Netherlands) and FRA 2 μ-AUTOLAB Type III (ECO CHEMIE Instruments B.V., Netherlands) were used for voltammetric, impedimetric and amperometric measurements. A three electrode cell where TM-Mont/*G. oxydans* electrodes as working electrode, Ag/AgCl electrode with 3.0 M KCl as a reference electrode and platinum (Pt) as the counter electrode were used. The FIA mode of analysis was performed using a single line flow injection manifold with an electrochemical flow through cell of the cross-flow type with an Ag/AgCl reference, Pt auxiliary (CHI130, Austin, USA) and glassy carbon working electrodes (GCE), a peristaltic pump (FIAtron, Oconomovoc, WI, USA) equipped with silicon tubing (0.89 mm inner diameter) pumped the working buffer solution as the carrier into the flow line at a flow rate of 0.9 mL min^{-1}.[33] The flow line was made of Teflon tubing (0.5 mm inner diameter). 50 μL sample solution containing substrate was injected into the carrier stream *via* an eight-port injection valve (FIAtron, Oconomovoc, WI, USA). The FIA system as shown in Scheme 1 was connected to a PalmSens potentiostat for the

This journal is © The Royal Society of Chemistry 2013

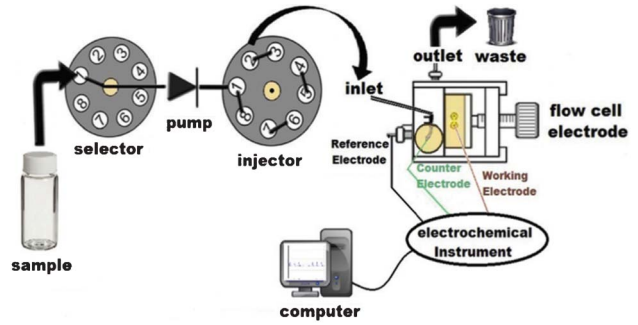

Scheme 1 Shematic representation of the established FIA based biosensing system.

Downloaded by Ege Universitesi on 03/04/2013 14:13:59.
Published on 07 March 2013 on http://pubs.rsc.org | doi:10.1039/C3RA40335A

electrochemical measurements. The FIA system was assisted by a software program written in C^{++} which was developed at the Institute for Technical Chemistry, Leibniz University (Hannover, Germany). Measurements of optical density for bacteria and a reference method for sample application were carried out with a T60U UV/VIS Spectrophotometer, (PG Ins. Ltd. Wibtoft, Leicestershire, UK). A Zeta-Meter 3.0+ (with Zeiss DR microscope, GT-2 type quartz cell, molybdenum-cylinder anode, and platinum-rod cathode electrode) was used for the zeta potential (ZP) analysis. Modified Mont was suspended in distilled water by stirring overnight. In electrophoresis, the particles were migrated by applying an electric field across the system. The microspheres were timed for both directions of the applied electric field. The value of the ZP assigned to the dispersions was the average of the data obtained from 10 experiments. The applied voltage during the measurements was varied in the range 20–30 mV. The ZP of the modified Mont suspensions was estimated from the measured electrophoretic mobility by employing the Smoluchowski equation. The electrokinetic charge densities were also calculated according to Yalcinkaya and Guler, 2010.[34] Fourier transform infrared spectroscopy (FTIR) spectra of pristine clay and modified clay were obtained using a Pyris 1 FTIR Spectrometer (Perkin–Elmer Instruments) on KBr plates. Thermal stability of the pristine clay and modified clay was studied by thermal gravimetric analysis (Perkin–Elmer TGA/DTA) from room temperature to 1000 °C, at a heating rate of 10 °C min^{-1} under an air atmosphere. X-ray diffraction (XRD) with a Philips E'xpert Pro diffractometer (Cu-Kα ray, λ = 1.54 Å) was used to calculate the basal spacing of unmodified and modified clays. The spacing values of Mont mineral were calculated by Bragg's law. All of the products were dried in a vacuum oven before the analyses. The surface morphology of the biofilm was investigated by scanning electron microscopy (SEM) analysis (Quanta FEG 250, Fei).

Clay modification

The modified clay was prepared by a cation exchange method, which involves the reaction between sodium cations of Mont and quaternary alkyl-ammonium ions of TM chloride which was used as an intercalating agent. Typically, Mont (5.0 g) was stirred in 600 mL of distilled water (beaker A) at room temperature overnight. An equivalent amount of cation exchange capacity (CEC) of Mont, containing 0.02 mmol of intercalating agent was put in another 50 mL of distilled water (beaker B) and stirred while 1.0 M HCl aqueous solution was added to adjust the pH to 3.0–4.0. After stirring for 3 h, the protonated amino acid solution (beaker B) was added slowly with vigorous stirring to the Mont suspension (beaker A). The mixture was stirred overnight at room temperature. The modified clay (TM-Mont) was then, recovered by ultracentrifugation (at 15 000 rpm for 15 min). Afterwards filtration was performed *via* a Buchner funnel. Purification of the products was carried out by washing and filtering the samples at least five times to remove any excess of ammonium ions. The modified clay was then obtained and used for the characterization and biosensing experiments.

Construction of biosensor

In order to construct the TM-Mont microbial layer, firstly GCE was polished with alumina slurry (0.05 μm sized) and then ultrasonication was applied for approximately 5 min in ethanol : distilled water (1 : 1) solution. Subsequently, 5.0 μL of Mont solution (1.0 mg mL^{-1} in PBS), 5.0 μL of *G. oxydans* suspension, 2.5 μL of BSA (1.0 mg mL^{-1} in PBS) and 1.0 μL of GA (1.0% in PBS) were mixed. Afterwards, the mixture was dropped onto the electrode and allowed to dry at room temperature for 1 h. In the FIA system the preparation conditions were the same and mixture was spread over the surface of the GCE in the flow cell.

Electrochemical measurements

All amperometric experiments in the batch mode were carried out in 10 mL buffer solution. Electrodes were rinsed with distilled water and kept in sodium phosphate buffer (50 mM, pH 6.5) for 3 min after each measurement. Bacteria immobilized electrodes were initially equilibrated in buffer and then, glucose was added to the reaction cell. The decrease in the oxygen amount as a result of metabolic activity was monitored at −0.7 V *vs.* Ag/AgCl. The electrode responses were registered as the current signal (μA). Buffer was refreshed after each measurement. All chronoamperometric measurements were performed 3 times. Data were presented as the mean ± standard deviation (S.D).

Cyclic voltammetric (CV) experiments and electrochemical impedance spectroscopy (EIS) measurements were performed on a FRA 2 μ-AUTOLAB Type III electrochemical measurement system from ECO CHEMIE Instruments B.V., (Netherlands) driven by GPES software (www.ecochemie.nl). EIS measurements were performed in sodium phosphate buffer (50 mM, pH 6.5) containing 5.0 mM $Fe(CN)_6^{3-/4-}$ with a frequency range from 0.01 Hz to 10 kHz at 0.2 V. CV measurements were conducted in the potential range of −0.4 V to 0.6 V with a 0.0244 V step potential in the presence of 1.0 mM KCl used as the supporting electrolyte.

Sample application

The TM-Mont/*G. oxydans* biosensor was applied in the determination of glucose in some beverages (coke, fizzy and cherry juice samples). Trinder reagent which is a commercial enzyme assay kit based on spectrophotometric analysis was used for independent glucose analysis. This reaction includes

Downloaded by Ege Universitesi on 03/04/2013 14:13:59.
Published on 07 March 2013 on http://pubs.rsc.org | doi:10.1039/C3RA40335A

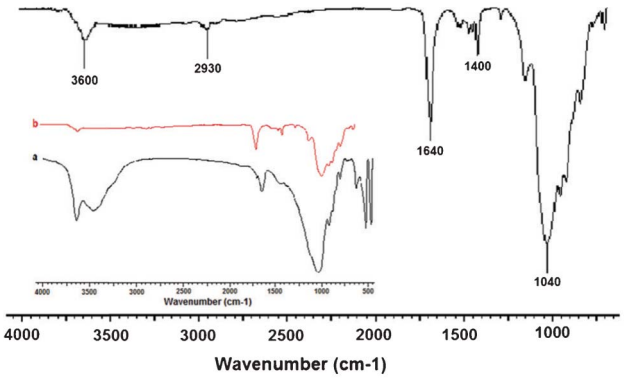

Fig. 1 FT-IR spectrum of TM-Mont [inset: pristine Mont (a) and TM-Mont (b)].

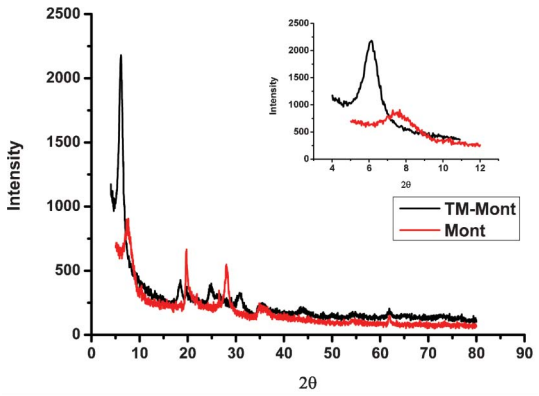

Fig. 2 Typical XRD patterns of Mont and TM-Mont.

oxidation of glucose to D-gluconate catalyzed by glucose oxidase with the formation of hydrogen peroxide. In the presence of peroxidase, a mixture of phenol and 4-aminoantipyrine is oxidized by hydrogen peroxide to form a red quinine imine dye proportional to the glucose concentration in the sample.[35]

Results and discussion

Surface characterization

Clay modification was characterized by using XRD, FTIR, TGA and ZP measurements. Intercalation of amine groups to the structure was confirmed by FTIR (Fig. 1). In the spectrum of Na-Mont in Fig. 1 (a), the silicon–oxygen bond was observed at 1040 cm^{-1}. The strong peak at 1640 cm^{-1} and the broad band at 3451 cm^{-1} have been assigned to the bending and stretching modes of adsorbed water. Sharp peaks around 3600 cm^{-1} were assigned to the hydroxyl group. In addition to these bands in Fig. 1 (b), the bands around 1400 cm^{-1} were attributed to the presence of N–H on the structure. C–H stretching bands of methyl- group and also N–CH_3 stretching bands were assigned at about 2930 cm^{-1}.

The structure of TM-Mont was characterized by XRD and compared with that of Mont. An X-ray diffractogram of Na-Mont is presented in Fig. 2. The basal spacing value (d_{001}) of Mont was calculated as 11.4 Å. For the TM-Mont, the basal spacing was expanded to 14.66 Å. The increase of the basal spacing values indicates that the sodium cations in the interlayer galleries of the clay were replaced by TM. This diffractogram shows shifting of the d-spacing of the TM modified Mont to lower diffraction angles by comparison to the unmodified Mont. Due to the increase of the interlayer distance of the Mont, an increasing of the basal spacing values of Mont was clearly seen. It is evident that the TM salts entered the interlayer of the clay. The higher extent of intercalation corresponds to the larger interlayer distance of 3.2 nm in TM-Mont which is due to its branched structure in comparison to M and DM intercalated Mont which was used in the previous work.[27]

The TGA thermograms of Mont and TM-Mont are shown in Fig. S1, ESI.† Mont exhibited about 8.4 wt% weight loss at 1000 °C. Degradation started at 100 °C due to the unbound H_2O and continued up to about 800 °C due to the chemically bound H_2O. For TM-Mont, the weight loss occured from 100 to 750 °C which is due to degradation of the TM salt and decomposition of the clay mineral. The weight loss of TM-Mont was found to be 23.4 wt% due to the presence of TM as a modifier. Hence, it was indicated that 15 wt% modifier was present on the Mont structure. This result was compatible with the calculated amount of modifier from CEC of the Mont. From the TGA results, it is obvious that the maximum weight loss was obtained with TM-Mont rather than M and DM intercalated Mont.[27]

The electrokinetic properties of particles in an aqueous solution play a significant role in understanding the adsorption mechanism of inorganic and organic species at the solid–solution interface. These properties vary depending on the surface potential and the thickness of the electrical double layer. ZP were calculated as -42.0 ± 2.24 and -28.1 ± 1.84 mV for Mont and TM-Mont from the Smoluchowski equation, respectively. After modification of Mont with TM salt, as a result of adsorption at the surface or interlayer of the mineral, the ZP shifted to less-negative values, due to the presence of positively charged amine salts. TM-Mont exhibited lower negative ZP values compared to that of the M and DM intercalated Mont due to the higher electronegativity of the nitrogen atom. This result was supported by electrokinetic charge densities which were calculated as -33.1 ± 2.24 and -19.2 ± 1.38 Cm^{-2} for Mont and TM-Mont, respectively. Application of various characterization techniques provided strong evidence that amine groups are distributed into the structure of Mont. Additionally Mont, M and DM intercalated Monts were prepared as previously reported[27] and some characteristics of these clay structures are summarized in Table S1, ESI.†

Electrochemical characterization

EIS is a useful technique for examining the change in surface electrochemistry. In the Nyquistic diagrams, the semicircle part at higher frequencies corresponds to the electron-transfer-limiting electrochemical process while the linear part at lower frequencies corresponds to the diffusion-controlled electrochemical process. The semicircle diameter on the other

This journal is © The Royal Society of Chemistry 2013

Published on 07 March 2013 on http://pubs.rsc.org | doi:10.1039/C3RA40335A
Downloaded by Ege Universitesi on 03/04/2013 14:13:59.

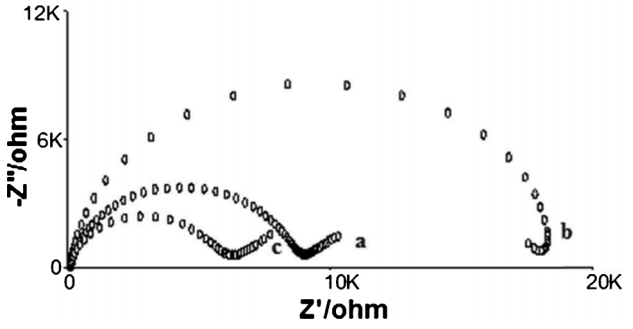

Fig. 3 Nyquistic plot of EIS for bare GCE (a), Mont modified GCE (b) and TM-Mont modified GCE (c) in the presence of 5.0 mM Fe(CN)63-/4- and 1.0 mM KCl in 50 mM sodium phosphate buffer (pH 6.5) at 0.2 V between 0.01 Hz- 10 kHz. [Configuration of the electrode surface: 5.0 μL *G. oxydans*, 5.0 μL clay (1.0 mg mL^{-1} in pH 7.4, PBS buffer), 2.5 μL BSA (1.0 mg mL^{-1} in pH 7.4 PBS buffer) and 1.0 μL GA (1.0% in pH 7.4, PBS buffer)].

hand, demonstrates the interfacial electron transfer resistance.[36] Fig. 3 shows the EIS responses of plain GCE (a), Mont (b) TM-Mont (c) modified GCEs in 5.0 mM $Fe_3(CN)_6^{3-/4-}$ As can clearly be seen from the Nyquistic diagram, TM-Mont-GCE has a smaller semi-circle diameter compared to Mont-GCE, demonstrating more efficient electron transfer of TM-Mont-GCE. This result is in agreement with ZP measurements (Fig. 3). Since TM-Mont has a smaller ZP which corresponds to a thinner electrochemical double layer, the electron transfer will be easier in this system. On the other hand, the bare GCE shows better electron transfer kinetics compared to the Mont-GCE. As a result it can be concluded that in electrochemical systems, it is beneficial to use TM-Mont-GCE rather than Mont-GCE.

CV measurements were also conducted to investigate the electrochemical mechanism in more detail. With Mont-GCE, ΔEp and E^0 values were found to be 0.62 and 0.25 mV respectively for 5.0 mM $Fe_3(CN)_6^{3-/4-}$. After the modification with TM, these values become 0.49 mV with E^0 of 0.24 mV. The decrease in ΔEp values demonstrates faster electron transfer kinetics than is obtained with the TM-Mont-GCE (data not shown). The effect of scanning rate on the cyclic voltammograms was also examined (Fig. 4). As a result, it has been observed that both systems have a linear semi diffusion controlled electron transfer between scan rates of 5.0–100 mV s^{-1}. Linear graphs for the anodic and cathodic peak currents *vs.* the square root of the scanning rates were defined by the following equations; for Mont/ GCE/*G. oxydans*, anodic and cathodic linear equations are $y = 1.843x + 7.658$ ($R^2 = 0.993$) and $y = 1.352x + 8.717$ ($R^2 = 0.988$), for TM-Mont/ GCE/*G. oxydans*, anodic and cathodic linear equations are $y = 0.816x + 7.743$ ($R^2 = 0.999$) and $y = 1.335x + 7.221$ ($R^2 = 0.980$). At higher scan rates, the current values obtained deviate from linearity.

Additionally, surface morphologies of the TM-Mont film and TM-Mont/*G. oxydans* film were imaged by SEM and are shown in Fig. S2 (a) and (b), ESI.†

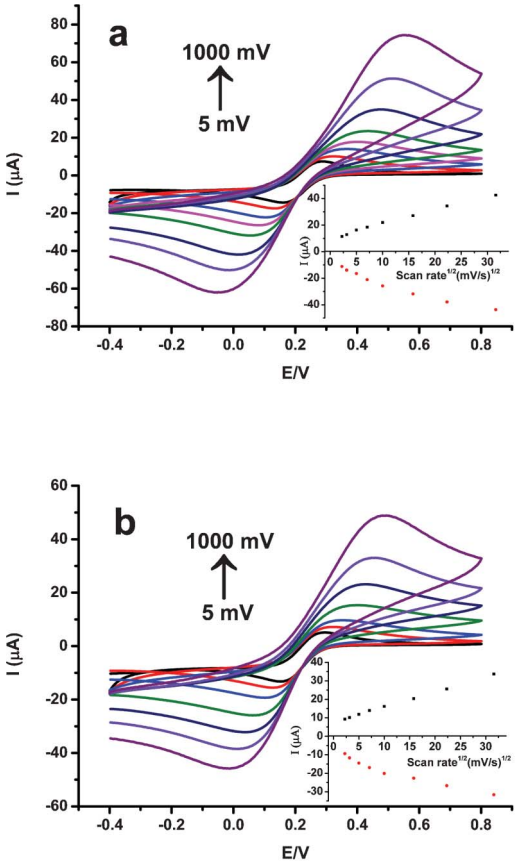

Fig. 4 Cyclic voltammograms of Mont/G. oxydans (a) and TM-Mont/*G. oxydans* (b). Measurement medium and electrode composition are the same as for Fig. 3. [Inset graphs show the correlation between the current and square of the scan rates (5.0; 10; 25; 50; 100; 250; 500; 1000 mV s^{-1})].

Optimization of the microbial sensor

Influences of pH and modifier type were investigated in batch configuration. The effect of pH on the response of the TM-Mont/*G. oxydans* biosensor was observed between pH 6.0 and 7.5 in 50 mM sodium phosphate buffer. The optimum pH value of the biosensor was found to be 6.5. This value is close to the pH of the cultivation medium which is reported to be pH 5.5–6.0.[7] On the other hand, the optimum pH mainly depends on the charge of the matrices used for the immobilization. In the previous report where *G. oxdans* were immobilized on the chitosan matrix, the optimum pH was found to be 7.0.[11] Afterwards, as well as TM-Mont, pristine Mont and M, DM intercalated Monts were used for the microbial sensor construction and the effect of modifier types on the current response were assessed in the presence of 0.5 mM glucose. The highest response was obtained with TM intercalated Mont (Fig. S3, ESI†). A more expanded basal spacing (14.66 Å) was obtained when the sodium cations in the interlayer galleries were replaced by TM in comparison to the other clay structure. Therefore, bacterial cells can be easily adhered onto the rough matrix. On the other hand, this structure caused higher oxygen availability for the metabolic activity and had good electron transfer properties.

Downloaded by Ege Universitesi on 03/04/2013 14:13:59.
Published on 07 March 2013 on http://pubs.rsc.org | doi:10.1039/C3RA40335A

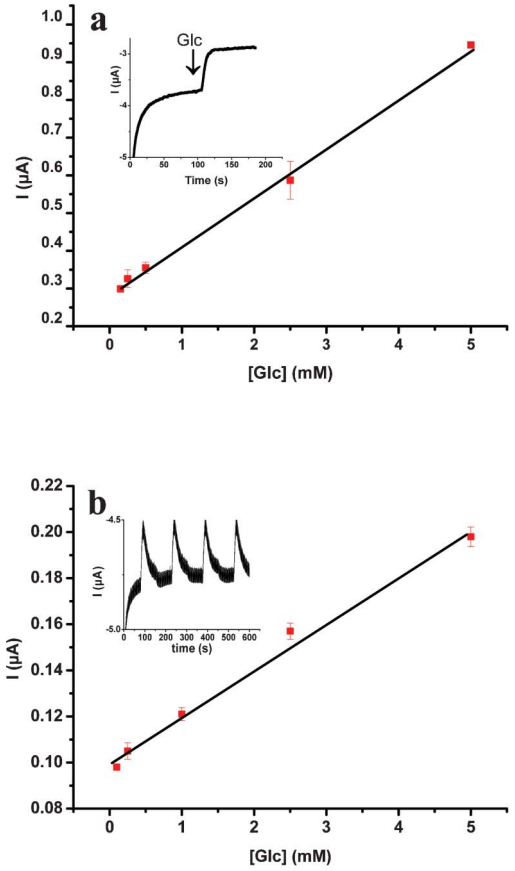

Fig. 5 Calibration curve for TM-Mont/G. oxydans biosensor in batch system (a) and FIA system (b) (insets: current–time curves, batch (a) and FIA (b)). Peaks obtained at the TM-Mont/G. oxydans biosensor with the successive addition of 5.0 mM glucose; −0.7 V; 50 mM sodium phosphate buffer (pH 6.5), at room temperature. Electrode composition is the same as for Fig. 3.

Analytical characteristics

Initially, the microbial sensor was calibrated to glucose, under the optimum experimental conditions in both batch and FIA modes. Linearity was obtained between 0.15 and 5.0 mM with 15 s response time in the batch system and is described by the following equation: $y = 0.131x + 0.283$, $R^2 = 0.997$. When the microbial sensor was applied in the FIA mode, linearity was obtained between 0.1 mM and 5.0 mM with an equation of $y = 0.020x + 0.0999$, ($R^2 = 0.990$) and with 70 s as response time, respectively (Fig. 5 (a) and (b)). Biosensor responses in both configurations were also given as insets of Fig. 5 (a) and (b).

The linearity of the TM-Mont/*G. oxydans* sensor is comparable to the previous *G. oxydans* sensors based on different immobilization strategies reported in the literature (Table 1). Therefore, it can be claimed that TM-Mont/*G. oxydans* sensors have a wide linearity with a fast response time (15 s for batch mode) and can be successfully applied in the FIA configuration to provide easy operation as well as computer controlled automated measurements as shown in previous work.[37,38,14]

Operational stability was examined at ambient conditions using 0.25 mM glucose in the FIA system (Fig. S5, ESI†). During 3 h, 72 subsequent injections were performed and a 27.1% decrease in the response was observed. Repeatability was also carried assessed. According to the results of 10 subsequent measurements in the FIA mode using 1.0 mM glucose, the ±S.D and coefficient of variation (c.v) were calculated to be ±0.038 and 3.79%.

Substrate specificity

G. oxydans contains many membrane-bound dehydrogenases such as alcohol, aldose and glycerol dehydrogenase. Due to the presence of these enzymes in *Gluconobacter sp.*, substrate specificity was studied using ethanol, fructose and glycerol. In this part, two different cell cultures were prepared using glucose (1.0 mM) and glycerol (1.0 mM) as the main carbon sources. After that, cells were harvested and used for the biosensor preparation. The sensor responses were given as current (I/μA) and are shown in Fig. S5, ESI.† Glucose gives the highest current value. Besides fructose, glycerol and ethanol also have similar responses when the bacteria have been grown in glucose. The highest current value for glucose was also observed when glycerol was used as the main carbon source. In that case ethanol, glycerol and fructose also gave signals but glucose and ethanol showed higher current values compared to other substrates. This might be due to the activation of alcohol dehydrogenases in the presence of glycerol in the culture medium. In a previous work, responses of a microbial sensor that was constituted with arabitol (polyalcohol like glycerol) cultivated cells were highest when glucose was put in the measurement medium.[39]

A glycerol calibration curve was also drawn using glycerol cultivated cells in the microbial sensor and the linear range was found to be between 0.5 and 10 mM glycerol and is defined by the following equation: $y = 0.008x + 0.070$, ($R^2 = 0.999$) with an 80 s response time (Fig. S6, ESI†). According to the response characteristics, it is obvious that the microbial sensor could be practically used for different analytes such as glycerol and ethanol as well as glucose after chromatographic separations.

Sample analysis

The constructed biosensor system was used for glucose analysis in some beverages such as coke, fizzy and cherry juice using the FIA configuration. Samples diluted with the carrier buffer were injected instead of the substrate and the glucose contents were calculated using the signals from the glucose calibration curve and are shown in Table 2. The accuracy of the analysis was tested using a spectrophotometric method for the same samples. Each data was given as the mean of 3–5 measurements ±S.D. According to the recovery values, this system can be used in sample application without needing any sample pre-treatment steps.

Table 2 Glucose content of some beverages obtained by the biosensor and the reference method

Sample	TM-Mont/*G. oxydans*/M	Trinder reagent/M	Recovery (%)
Coke	0.286 ± 0.07	0.289 ± 0.06	98.9
Fizzy	0.291 ± 0.13	0.29 ± 0.0	100.3
Cherry Juice	0.419 ± 0.48	0.416 ± 0.11	100.7

This journal is © The Royal Society of Chemistry 2013

Downloaded by Ege Universitesi on 03/04/2013 14:13:59.
Published on 07 March 2013 on http://pubs.rsc.org | doi:10.1039/C3RA40335A

Conclusions

Clays generate available matrices for biological applications in which biomolecules need to be immobilized on surfaces. The fast and easy immobilization properties of clays such as Mont, laponite and layered double hydroxides have been used for the preparation of many enzyme biosensors and allow sensitive measurements to be made.[40–43] The developed TM-Mont/*G. oxydans* sensor has shown good linearity in both configurations (batch and FIA) with good repeatability. The substrate specificity was also investigated with glucose and glycerol cultivated cells. Finally, sample analysis showed that Mont based microbial sensors could be suitable for easy and practical measurements with good accuracy.

References

1 S. Cosnier, F. Lambert and M. Stoytcheva, *Electroanalysis*, 2000, **12**, 356–360.
2 P. K. Ghosh and A. J. Bard, *J. Am. Chem. Soc.*, 1983, **105**, 5691–5693.
3 E. E. Saka and C. Guler, *Clay Miner.*, 2006, **41**, 853–861.
4 M. M. Collinson, *TrAC, Trends Anal. Chem.*, 2002, **21**, 30–38.
5 S. F. D'Souza, *Biosens. Bioelectron.*, 2001, **16**, 337–353.
6 K. Riedel, in *Enzyme and Microbial Biosensors: Techniques and Protocols*, ed. A. Mulchandani and K. R. Rogers, Humana Press, Totowa, NJ, 1998, pp. 199–223.
7 A. Gupta, V. K. Singh, G. N. Qazi and A. Kumar, *J. Mol. Microbiol. Biotechnol*, 2001, **3**, 445–456.
8 K. A. Lusta and A. N. Reshetilov, *Prikl. Biokhim. Mikrobiol.*, 1998, **34**, 339–353.
9 S. Macauley, B. McNeil and L. M. Harvey, *Crit. Rev. Biotechnol.*, 2001, **21**, 1–25.
10 S. Tuncagil, D. Odaci, E. Yildiz, S. Timur and L. Toppare, *Sens. Actuators, B*, 2009, **137**, 42–47.
11 D. Odaci, S. Timur and A. Telefoncu, *Bioelectrochemistry*, 2009, **75**, 77–82.
12 J. Sefcovicova, J. Filip, V. Mastihuba, P. Gemeiner and J. Tkac, *Biotechnol. Lett.*, 2012, **34**, 1033–1039.
13 E. Baskurt, F. Ekiz, D. Odaci Demirkol, S. Timur and L. Toppare, *Colloids Surf., B*, 2012, **97**, 13–18.
14 O. Yilmaz, D. Odaci Demirkol, S. Gulcemal, A. Kilinc, S. Timur and B. Cetinkaya, *Colloids Surf., B*, 2012, **100**, 62–68.
15 O. Habib, D. Odaci and S. Timur, *Food Anal. Methods*, 2011, **5**, 188–194.
16 M. Valach, J. Katrlik, E. Sturdik and P. Gemeiner, *Sens. Actuators, B*, 2009, **138**, 581–586.
17 I. Vostiar, E. E. Ferapontova and L. Gorton, *Electrochem. Commun.*, 2004, **6**, 621–626.
18 A. N. Reshetilov, P. V. Iliasov, M. V. Donova, D. V. Dovbnya, A. M. Boronin, T. D. Leathers and R. V. Greene, *Biosens. Bioelectron.*, 1997, **12**, 241–247.
19 J. Tkac, I. Vostiar, L. Gorton, P. Gemeiner and E. Sturdik, *Biosens. Bioelectron.*, 2003, **18**, 1125–1134.
20 J. Katrlik, I. Vostiar, J. Sefcovicova, J. Tkac, V. Mastihuba, M. Valach, V. Stefuca and P. Gemeiner, *Anal. Bioanal. Chem.*, 2007, **388**, 287–295.
21 L. N. Warr, J. N. Perdrial, M. Lett, A. Heinrich-Salmeron and M. Khodja, *Appl. Clay Sci.*, 2009, **46**, 337–345.
22 X. Mao, J. Wang, A. Ciblak, E. E. Cox, C. Riis, M. Terkelsen, D. B. Gent and A. N. Alshawabkeh, *J. Hazard. Mater.*, 2012, **213–214**, 311–317.
23 Z. Sarcheshmehpour, A. Lakzian, A. Fotovat, A. R. Berenji, G. H. Haghnia and S. A. Seyed Bagheri, *Hydrometallurgy*, 2009, **98**, 33–37.
24 F. W. Welsh, R. E. Williams and I. A. Veliky, *Enzyme Microb. Technol.*, 1987, **9**, 500–502.
25 B. Müller, *Geoderma*, 2009, **153**, 94–103.
26 C. Mousty, *Appl. Clay Sci.*, 2004, **27**, 159–177.
27 M. Seleci, D. Ag, E. E. Yalcinkaya, D. Odaci Demirkol, C. Guler and S. Timur, *RSC Adv.*, 2012, **2**, 2112–2118.
28 Q. Fan, D. Shan, H. Xue, Y. He and S. Cosnier, *Biosens. Bioelectron.*, 2007, **22**, 816–821.
29 J. Chen and Y. Jin, *Bioelectrochemistry*, 2011, **80**, 151–154.
30 C. Lei and J. Deng, *Anal. Chem.*, 1996, **68**, 3344–3349.
31 S. Poyard, N. Jaffrezic-Renault, C. Martelet, S. Cosnier, P. Labbé and J. L. Besombes, *Sens. Actuators, B*, 1996, **33**, 44–49.
32 C. Gatgens, U. Degner, S. Bringer-Meyer and U. Hermann, *Appl. Microbiol. Biotechnol.*, 2007, **76**, 553–559.
33 M. Akin, A. Prediger, M. Yuksel, T. Höpfner, D. Odaci Demirkol, S. Beutel, S. Timur and T. Scheper, *Biosens. Bioelectron.*, 2011, **26**, 4532–4537.
34 E. E. Yalcinkaya and C. Guler, *Sep. Sci. Technol.*, 2010, **45**, 635–642.
35 P. Trinder, *Ann. Clin. Biochem.*, 1969, **6**, 24–27.
36 U. Anik, S. Cevik and S. Timur, *Electroanalysis*, 2011, **23**, 2379–2385.
37 M. Akin, M. Yuksel, C. Geyik, D. Odaci, A. Bluma, T. Höpfner, S. Beutel, T. Scheper and S. Timur, *Biotechnol. Prog.*, 2010, **26**, 896–906.
38 M. Yuksel, M. Akin, C. Geyik, D. Odaci Demirkol, C. Ozdemir, A. Bluma, T. Höpfner, S. Beutel, T. Scheper and S. Timur, *Biotechnol. Prog.*, 2011, **27**, 530–538.
39 J. Tkac, P. Gemeiner, J. Svitel, T. Benikovsky, E. Sturdik, V. Vala, L. Petrus and E. Hrabarova, *Anal. Chim. Acta*, 2000, **420**, 1–7.
40 L. Fernandez and H. Carrero, *Electrochim. Acta*, 2005, **50**, 1233–1240.
41 D. Shan, S. Cosnier and C. Mousty, *Biosens. Bioelectron.*, 2004, **20**, 390–396.
42 P. Y. Liang, P. W. Chang and C. M. Wang, *J. Electroanal. Chem.*, 2003, **560**, 151–159.
43 S. Cosnier and K. Le Lous, *Talanta*, 1996, **43**, 331–337.